SEISMIC TUNNEL IMAGING AND DETECTION

Ali C. Gurbuz, James H. McClellan, Waymond R. Scott, Jr.

Georgia Institute of Technology
Electrical and Computer Engineering
Atlanta, GA

Gregg D. Larson

Georgia Institute of Technology
Mechanical Engineering
Atlanta, GA

ABSTRACT

To investigate the problem of detecting and imaging underground tunnels, an experimental system that utilizes seismic waves has been constructed. Seismic reflections from the tunnel are transformed into a 3D image using a synthetic aperture time-delay backprojection algorithm. Results from experimental data show that the tunnel is directly visible in the backprojected image. Nevertheless, tunnels with low signal to noise ratio (SNR) are located using 2D and 3D Radon Transforms followed by a detection algorithm. A simulation is performed on the performance of the Radon transform for detecting lines in noisy images and it is shown how lines in very low SNR images can be detected. Also it is observed that longer lines have higher probability of detection at the same noise level.

Index Terms— Radon transforms, Seismic signal processing, Seismic measurements, Tunnel detection, Seismic imaging.

1. INTRODUCTION

Seismic exploration is one of the most popular and successful methods for imaging the earth's interior. Seismic waves are used in a broad spectrum of applications ranging from oil and gas prospecting [1] to imaging land mines [2, 3]. A seismic wave transmitted through the air and soil reflects from subsurface targets and can be received by sensors on the ground. The record of these reflections is used by an imaging or detection algorithm to localize or image the subsurface targets.

Previous research on tunnel imaging has mainly focused on the design and development of data collection systems. Electromagnetic and seismic techniques are commonly used. While research on electromagnetic techniques focuses on crosshole tomography [4], seismic techniques often use reflection systems [5], and emphasize seismic signal characterization [6]. In this paper, we focus on seismic image formation and image processing techniques.

To investigate the applicability of seismic waves to tunnel imaging, seismic image formation and image processing techniques, a laboratory scale experimental model is developed at the Georgia Institute of Technology [2]. Seismic reflections from the model tunnel are transformed to 3D spatial images using a time domain synthetic aperture backprojection algorithm (Section 3). To extract and detect linear features in the backprojected image, the Radon transform is applied. Performance of the Radon transform in varying noise levels is studied and it is shown that lines which cannot be visually seen in the backprojected images can be detected after the Radon transform. Additionally, longer lines have a higher probability of detection at the same noise level.

The next section explains the experimental seismic system, data collection and data structure. Section 3 reviews seismic image formation techniques. Radon transformation results and performance analysis of the Radon transform in noise is given in Section 4.

2. SEISMIC DATA COLLECTION SYSTEM

Measurements to seismically detect a shallow subsurface tunnel were conducted in an experimental model in a laboratory at Georgia Tech [2, 3] using a midwoofer as the acoustic source and the accelerometer as the surface-contacting sensor as shown in Fig.1(a). The source and sensor were scanned over a 1.8 m by 1.8 m region in 4 cm increments by an automated positioning system. To simulate a shallow tunnel, a 3 m long, 10 cm diameter, corrugated drainage pipe was buried approximately 58 cm deep in the experimental model parallel to the y-axis at $x = 0$ cm.

Data acquisition and signal generation were accomplished at 32,000 points/second with a 4 second chirp excitation over frequencies from 100 Hz to 8 kHz. The chirp excitation was low-pass filtered at 8 kHz with appropriate amplification. Compression of the data using a 2.4 kHz center frequency differentiated Gaussian pulse in the post-processing results in the hyperbolic tunnel signature seen in Fig.1(b). The hyperbolic signature of the tunnel can be clearly seen in the image.
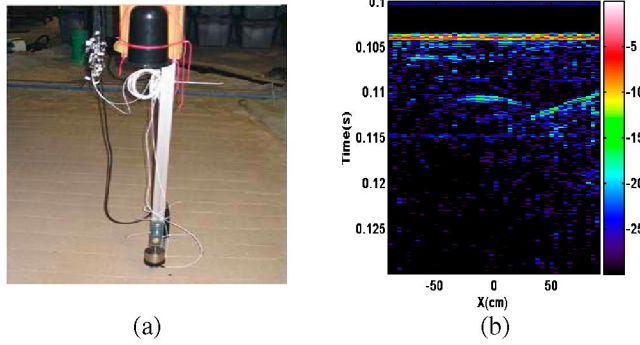
Fig. 1. (a) Seismic Data Collection System, (b) Measured raw data over a cross section of the tunnel.

3. SEISMIC IMAGING

The response of a synthetic aperture data acquisition process for a point target is a spatially variant hyperbolic curve that may be transformed into an image with the standard backprojection [7] algorithm. This algorithm performs matched filtering at each point in space using the impulse response of the data acquisition process. Even though tunnels are not point-like targets, as an initial method of processing we applied time-domain standard backprojection to the seismic data. The imaging algorithm can be formulated as follows:

$$f(x_n, y_n, z_n) = \int \int w(u_x, u_y) d(u_x, u_y, t) \delta(t - \frac{d_T}{c}) dt du_x du_y \tag{1}$$

where $d(u_x, u_y, t)$ is the measured seismic space-time data, $w(u_x, u_y)$ is the aperture weighting function, $f(x_n, y_n, z_n)$ is the subsurface image, and d_T is the total distance from the source to the imaging point (x_n, y_n, z_n) and back to the receiver. The speed of the seismic pressure wave in the medium is denoted by c and is measured to be $177m/s$. This value is assumed constant over the medium. Applying (1) to the mea-

obtained as different images of the tunnel. Figure 2(b) shows a slice of the backprojected image that corresponds to the raw data slice shown in Fig. 1(b). The tunnel is visibly quite pronounced in the backprojected images. Figure 2(a) image is formed by summing the energy values over all depths. The two linear structures in the image are the tunnel and the sloped part of side of the sandbox. Figure 4 shows the iso-surface image of the tunnel.
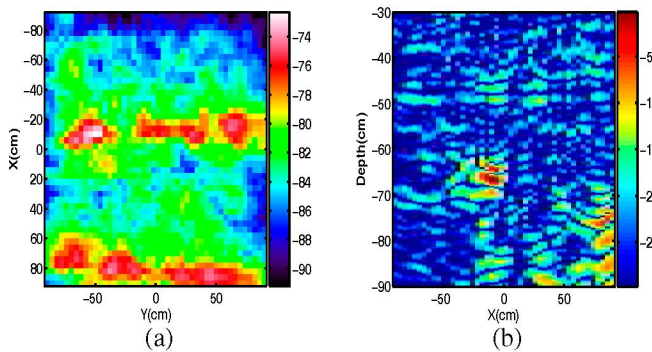
4. RADON TRANSFORM FOR DETECTION OF TUNNELS

The Radon transform [8] maps an image into a parameterized domain such that the parameterized shapes (lines and curves) correspond to a peak in the parameter domain. The Radon transform of a digital image $f(x, y)$ using the parametrization of a line can be given as follows:

$$R(m, n)[f(x, y)] = \int_{-\infty}^{\infty} f(x, mx + n) dx \tag{2}$$

where m and n are the slope and the intercept of the line, respectively. Since parameterized curves correspond to peaks in Radon space the Radon transform can be used as a tool for detection of curves in the images. For the specific application of tunnel imaging and detection, we model tunnels as lines over short distances; thus the problem of tunnel detection is converted to a problem of detecting the corresponding peak in the Radon space. Using a detection algorithm in radon space also enables us to simultaneously determine the line parameters .

Applying the Radon transform to Fig. 2(a), Fig. 3(a) is obtained. The lines corresponding to the peaks in the image are shown in Fig. 3(b). The Radon transform finds lines that correspond to the tunnel and the sloped part of the sandbox bottom easily. From the surface energy image, the depth in-

Fig. 2. (a) Surface energy image, (b) One slice of the backprojected data.

sured seismic data of the model tunnel area, Figs. 2 and 4 are
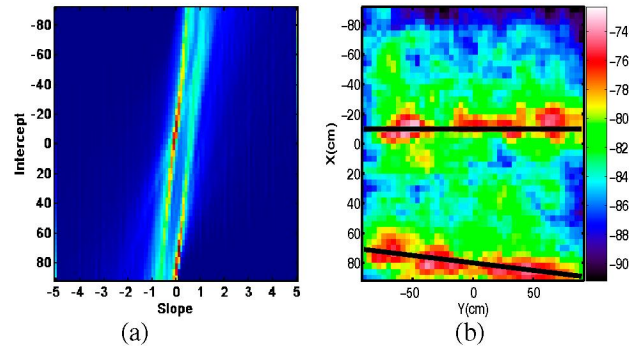
Fig. 3. (a) Radon Transform of the surface energy image, (b) Surface energy image and detected lines.

formation of the tunnel cannot be obtained. To determine how the tunnel is positioned on the z-axis, a 3-dimensional Radon

transform of the backprojected seismic image is taken. The line parametrization in 3D and the Radon transform can be found in [8]. Applying the 3D Radon transform to our back-projected data and taking the maximum peak in the parameter domain gives the line estimate shown in Fig. 4.
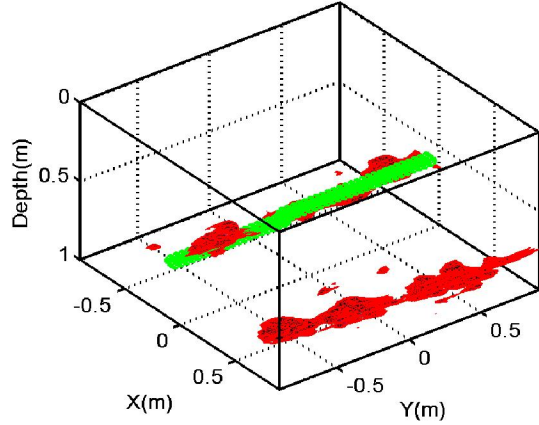
Fig. 4. Isosurface image of the backprojected data (-20dB level) with the detected line for the tunnel

4.1. Detection of Lines in Radon Transform Space

To develop a detection strategy, the following assumptions are made:

1. Images of size $L_i x L_i$ contain lines of average signal value μ_t and length L_t, where μ_t and L_t can be different for different lines in the image.

2. The image contains white Gaussian noise (WGN) of zero mean and variance σ^2 and the noise is uncorrelated with respect to the signal.

From (2), the Radon Transform makes a summation over lines in the image. The summation of the noise terms over the size of the image L_i will be Gaussian distributed with zero mean and variance $L_i\sigma^2$. The point in Radon space that corresponds to the line t in the image space will be also Gaussian distributed with mean $\mu_t L_t$ and variance $L_i\sigma^2$. Thus, the detection of lines in the images is actually equivalent to the detection of a constant level in WGN. The hypothesis for the detection test are

$$
\begin{aligned}
H_0 : & \quad R \sim N(0, L_i\sigma^2) \\
H_1 : & \quad R \sim N(\mu_t L_t, L_i\sigma^2)
\end{aligned}
\tag{3}
$$

The probability of detection for the Neyman-Pearson test is given by [9]

$$
P_D = Q(\frac{\gamma - \mu L_t}{\sqrt{L_i\sigma^2}})
\tag{4}
$$

where the threshold γ is selected according to the selected probability of false alarm, P_{FA}, as $\gamma = \sqrt{L_i\sigma^2}Q^{-1}(P_{FA})$. Figure 5(a) shows the receiver operating characteristics (ROC) plots for a 0 dB image of different line lengths in an image of size $L_i = 100$. We can see that longer lines have higher probability of detection for the same P_{FA}. Figure 5(b) shows ROC curves for different SNR values for a line length of 20. Lines with higher SNR also have higher P_D at the same P_{FA}.
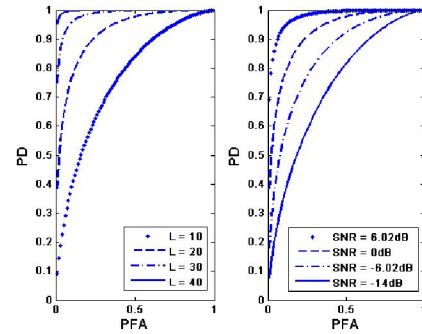
Fig. 5. (a) ROC Curves for fixed SNR = 0 and varying line lengths. (b) ROC curves for fixed Line length L = 20 and varying SNR levels.

4.2. Detection performance in Radon Space

One of the most important parameters for detecting lines in the images is the performance of the detection in varying noise levels. To determine the detection performance of the Radon transform a simulation is performed. The characteristics we are trying to observe are the probability of detection vs. SNR and the effect of line length on the probability of detection. Thus, a line is formed and white Gaussian noise with zero mean and varying variance level is added to the image. Here we assume that the noise and the signal are uncorrelated.

Figure 6 shows the same line in 4 different noise levels. The top left image is the sample line with no noise added. For the other images, Gaussian noise is added such that the SNR values are 10 dB, 0 dB and -6.02 dB respectively. The corresponding Radon transforms of the images are given in Fig. 7. As can be seen from all 4 images, the line in Radon space can be easily detected even though the lines in the images for SNR 0 dB or -6.02 dB cannot be visually identified.

To study how probability of detection changes as a function of SNR in Radon space, the simulation is repeated 500 times with random noise generation and the true line detection results are counted at each SNR value. The results are plotted in Fig.8. It can be observed from (4) and Fig. 8 that SNR and the line lengths has the following property

$$
\frac{\sqrt{SNR_1}}{\sqrt{SNR_2}} = \frac{L_{t_1}}{L_{t_2}}
\tag{5}
$$
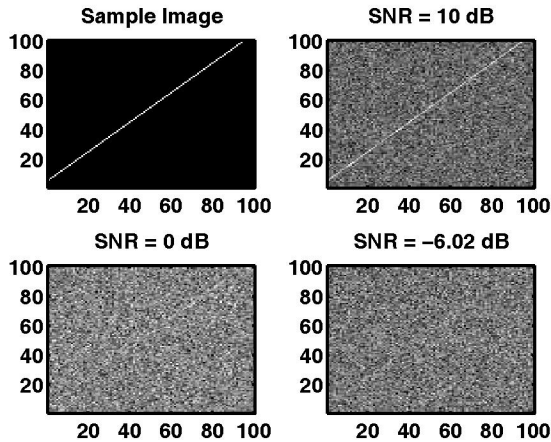
Fig. 6. Line image for different noise variances
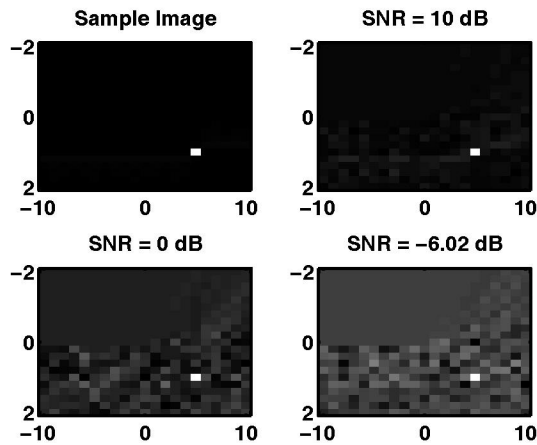
Fig. 7. Radon Transforms of the images in Fig. 6. Images are linear scale.

5. CONCLUSIONS

The imaging and detection of tunnels using seismic waves are demonstrated with a laboratory experimental model. Time domain backprojection is used for imaging reflected seismic data. The Radon transform is used as a tool for detecting tunnels in the backprojected images. Higher dimensional Radon transforms of the images are taken to find the position of the lines in all dimensions. A detection algorithm for line detection in Radon space is presented. The performance of the Radon transform to detect lines in varying noise levels is studied and it is observed that using the Radon transform; even invisible lines in low SNR images can be detected. It is also observed that lines with longer length have a higher probability of detection.
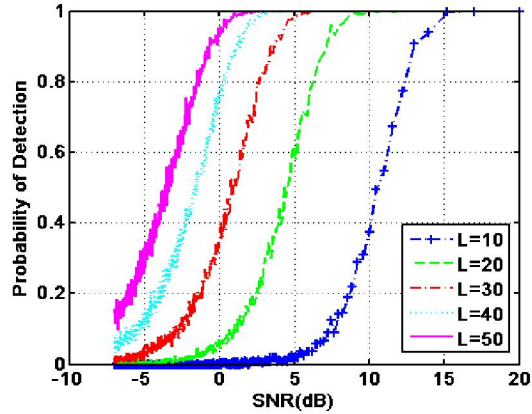
Fig. 8. P_D vs. SNR plot for line detection in Radon space

6. REFERENCES

[1] L.C. Wood and S.Treitel, "Seismic signal processing," in *Proceedings of the IEEE*, 1975, vol. 63, pp. 649 – 661.

[2] W.R. Scott, J.S. Martin, and G.D. Larson, "Experimental model for a seismic landmine detection system," *IEEE Transactions on Geoscience and Remote Sensing*, vol. 36, pp. 1155 – 1164, 2001.

[3] W.R. Scott, Kangwook Kim, G.D. Larson, A.C. Gurbuz, and J.H. McClellan, "Combined seismic, radar, and induction sensor for landmine detection," in *Geoscience and Remote Sensing Symposium*, 2004, vol. 3, pp. 1613 – 1616.

[4] S. Shope and R.J. Greenfield, "Electromagnetic cross-hole tomography for tunnel detection," in *Third Technical Symposium on Tunnel Detection Proceedings*, 1988, pp. 123–136.

[5] T.E. Owen, J.O. Parra, and J.T. O'Brien, "Shear-wave seismic reflection system for tunnel search and detection," in *Third Technical Symposium on Tunnel Detection Proceedings*, 1988, pp. 1–14.

[6] G.B. Hembree and G.H. Cabaniss, "Seismic signal characterization and analysis," in *Third Technical Symposium on Tunnel Detection Proceedings*, 1988, pp. 31–45.

[7] S-M. Oh, *Iterative space-time domain fast multiresolution SAR imaging algorithms*, Ph.D. thesis, Georgia Institute of Technology, Atlanta, GA, 2001.

[8] P. Toft, *The Radon Transform Theory and Implementation*, Ph.D. thesis, Technical University of Denmark, Lyngby, Denmark, 1996.

[9] S. M. Kay, *Fundamentals of Statistical Dignal Processing Detection Theory*, Prentice Hall, 1998.